

Navigating with highly precise odometry and noisy GPS: a case study *

Axel Barrau, Silvère Bonnabel

► **To cite this version:**

Axel Barrau, Silvère Bonnabel. Navigating with highly precise odometry and noisy GPS: a case study
*. 2016. <hal-01267244>

HAL Id: hal-01267244

<https://hal.archives-ouvertes.fr/hal-01267244>

Submitted on 9 Feb 2016

HAL is a multi-disciplinary open access archive for the deposit and dissemination of scientific research documents, whether they are published or not. The documents may come from teaching and research institutions in France or abroad, or from public or private research centers.

L'archive ouverte pluridisciplinaire **HAL**, est destinée au dépôt et à la diffusion de documents scientifiques de niveau recherche, publiés ou non, émanant des établissements d'enseignement et de recherche français ou étrangers, des laboratoires publics ou privés.

Navigating with highly precise odometry and noisy GPS: a case study*

Axel Barrau and Silvère Bonnabel †

Abstract

For linear systems, the Kalman filter perfectly handles rank deficiencies in the process noise covariance matrix, i.e., deterministic information. Yet, in a nonlinear setting this poses great challenges to the extended Kalman filter (EKF). In this paper we consider a simplified nonlinear car model with deterministic dynamics, i.e., perfect odometry, and noisy position measurements. Simulations evidence the EKF, when used as a nonlinear observer, 1- fails to correctly encode the physical implications of the deterministic dynamics 2- fails to converge *even for small* initial estimation errors. On the other hand, the invariant (I)EKF, a variant of the EKF that accounts for the symmetries of the problem 1- correctly encodes the physical implications of the deterministic information 2- is mathematically proved to (almost) *globally* converge, with explicit convergence rates, whereas the EKF does not even locally converge in our simulations. This study more generally suggests the IEKF is way more natural than the EKF, for high precision navigation purposes.

1 Introduction

The extended Kalman filter (EKF) has been developed by the NASA in the 1960s for the Appolo program. It has since been the state of the art for (industrial) navigation. The engineers appreciate its ease of implementation, its rather easy tuning based on the sensors' noises, and its optimal stochastic properties up to second order terms. Yet it is known to loose its properties when the initial errors become too large, due to the nonlinearities. As a result, over the past decade or so we have witnessed many attempts to derive alternative observers with asymptotic convergence properties for attitude and pose estimation. Those important properties - reserved to the deterministic setting - often use the Lie group structure of the state space, see, e.g., [11, 18, 3, 15, 12, 7, 17, 19, 4].

*This work is supported by the company Safran

†axel.barrau@mines-paristech.fr is with SAFRAN TECH, Groupe Safran, Rue des Jeunes Bois - Châteaufort, 78772 Magny Les Hameaux CEDEX. silvere.bonnabel@mines-paristech.fr is with MINES ParisTech, PSL Reasearch University, Centre for Robotics, 60 bd Saint-Michel, 75006 Paris, France.

The Invariant Extended Kalman Filter (IEKF) is a relatively recent variant of the EKF meant to account for the invariance/symmetries properties of the state space when devising EKFs on Lie groups, see [6, 5, 14, 2]. As such, it can be viewed as a variant of the multiplicative extended Kalman filter (MEKF) [8] for attitude estimation, and as an extension to it for pose estimation. It has the merit to retain all the EKF advantages - being a variant of it - while possessing a nicer geometric structure. In [1], local guaranteed convergence properties are derived for a large class of systems, and simulations indicate remarkable robustness to large initialization errors for high precision navigation problems. However no global property of the IEKF has ever been proved. The present paper allows to gain insight into the global IEKF properties by considering a simple example.

We study a non-holonomic car with perfect odometry and noisy position (i.e. GPS) measurements, where the initial position is known but not the orientation. This simplified navigation problem can be viewed as a limit case of high-accuracy navigation where inertial sensors allow precise navigation for several minutes in the absence of measurement. The degenerate situation of perfectly known dynamics poses no problem to the linear Kalman filter, the gains being possibly large at the beginning if the prior information is inaccurate, and then decreasing to zero. Yet, it poses great challenges to the EKF as gains can go to zero whereas, due to nonlinearities, the estimation error has not reduced enough, leading to a static asymptotic non-zero error, or divergence, even for unnoisy measurements. Note that, the general local convergence proof of [13] requires full rank process noise covariance, which is violated here. The usual remedy is either to artificially inflate the process noise covariance matrix, known as “robust tuning” (see [9, 16]) - but this results in degraded stochastic performance as the filter’s tuning does not match with the true sensors’ characteristics, or to use optimization methods over the first steps to initialize the EKF with a better guess of the true state. Note also, in passing, that as the state conditional probability does not have a density, even particle filters may face severe issues for the considered problem (the resampling step needs process noise to be useful). Here we show the nice geometric structure of the IEKF allows it to perfectly cope with the absence of process noise.

The main merit of the present paper is thus to show one can devise an EKF variant for a simple yet instructive navigation example, which possesses global properties both in terms of behavior and convergence. To our best knowledge this is the first time an EKF variant with global convergence properties is derived for an example of engineering interest, whereas the standard EKF does not even converge. Of course, the symmetries play a prominent role as they bring a lot of structure into the problem. The results obtained suggest great potential benefits of the IEKF over EKF for high precision navigation.

The contributions and organization of the paper are as follows. In Section 2 we recall the implications of deterministic dynamics in the linear case, and how the linear Kalman filter naturally encodes this information. We also introduce our simplified car model and derive the standard EKF equations for it. In Section 3, we discuss the physical implications of the choice of deterministic dynamics for the simplified car, and prove the IEKF naturally encodes this information, reminding the linear case: This is our main contribution. Finally, in Section 4, we leverage those results to derive some

global convergence properties of the IEKF for this problem.

2 Filtering with perfect odometry

2.1 The linear case

Consider in \mathbb{R}^n a deterministic continuous-time linear system $\dot{x}_t = A_t x_t$ with noisy discrete output measurements $Y_n = H_n x_{t_n} + V_n$ at times $t_1 < \dots < t_n$, where V_n is a Gaussian variable. Assume that initially part of the state is known, that is, for some matrix $\tilde{C} \in \mathbb{R}^{p \times n}$ we have $\tilde{C}x_0 = \alpha$ with $\alpha \in \mathbb{R}^p$ a known vector. This means that the state is initially known to be in a subspace of dimension $n - p$. By propagating this subspace through the deterministic dynamics, the state is known to be in a subspace of dimension $n - p$ at any time. Indeed letting $C_t \in \mathbb{R}^{p \times n}$ be the solution of $\dot{C}_t = -C_t A_t$ with $C_0 = \tilde{C}$, we have at all times $C_t x_t = \alpha$ as proved by differentiation.

A Kalman filter perfectly handles this kind of singular information about the state. Indeed, the fact that $C_0 x_0$ be initially perfectly known, means in probabilistic terms that there is no dispersion of the distribution of x_t orthogonally to the subspace the state lives in, and thus $C_0 P_0 C_0^T = 0$ where P_t denotes the covariance matrix output by the Kalman filter. This equality implies that at all times the estimate of the Kalman filter remains in the subspace the state lives in (if initialized inside it), and P_t keeps reflecting the absence of dispersion of the probability distribution of the state orthogonally to this subspace, as shown by the following trivial result. Note that the result in fact directly stems from the fact the filter computes the true probability distribution of the state conditioned on the outputs.

Proposition 1. *Consider the deterministic dynamics $\dot{x}_t = A_t x_t$ with noisy measurements $Y_n = H_n x_{t_n} + V_n$. If initially we have $C_0 x_0 = \alpha$, implying $C_t x_t = \alpha \forall t \geq 0$ where $\dot{C}_t = -A_t C_t$, then the linear Kalman filter is such that $C_t \hat{x}_t = \alpha \forall t \geq 0$. Moreover, the absence of dispersion orthogonally to the subspace the state lives in is correctly captured by the covariance matrix as $C_t P_t C_t^T = 0 \forall t \geq 0$.*

Proof. Between two measurements the Riccati equation $\frac{d}{dt} P_t = A_t P_t + P_t A_t^T$ implies $C_t P C_t^T = 0$, and when there is a measurement the covariance updates writes $P_{t_n}^+ = (I - K_n H_n) P_{t_n}$, and thus $C_{t_n} P_{t_n} C_{t_n}^T$ implies $C_{t_n} P_{t_n}^+ C_{t_n}^T$. Indeed, as P_{t_n} is symmetric, we have necessarily $C_{t_n} P_{t_n} = 0$ and thus $C_{t_n} K_n = 0$. The latter equality also implies the state is forced to remain in the subspace, as the update writes $\hat{x}_{t_n}^+ = \hat{x}_{t_n} + K_n (Y_n - H_n \hat{x}_{t_n})$. \square

2.2 Implications of perfect odometry for the nonlinear simplified car

Consider a non-holonomic car with deterministic dynamics (e.g. [10])

$$\begin{aligned} \frac{d}{dt} \theta_t &= \omega_t, \\ \frac{d}{dt} x_t &= \begin{pmatrix} \cos(\theta_t) u_t \\ \sin(\theta_t) u_t \end{pmatrix}, \end{aligned} \tag{1}$$

where θ_t is the heading of the car, x_t is the position vector, and ω_t, u_t are the angular and linear velocities computed through odometry. We also consider noisy position measurements. Those measurements can be interpreted as GPS measurements, or some other position measurements that arise in mobile robotics. Our goal is to understand what happens when the odometry becomes infinitely more precise than the other sensors, a situation that may arise in mobile robotics, and which also serves as a simplified problem for high precision inertial navigation. We thus consider noisy position measurements

$$Y_n = x_{t_n} + V_n, \quad (2)$$

where V_n is an i.i.d. Gaussian noise with covariance matrix R . Furthermore, we assume that the car's initial position is known, but its heading is not. As the state initially belongs to a one-dimensional submanifold of the state space, and the dynamics is perfectly known, it remains at all times in a one-dimensional submanifold one can compute.

Proposition 2. *Consider the dynamics (1). Assume the initial position is known, i.e., $x_0 = 0_{2,1}$. The dynamics being deterministic, at all times, the state (θ_t, x_t) belongs to the image of the set $S^1 \times \{0\} \times \{0\}$ through the flow of (1). This set being invariant to rotations, it can be parameterized in a more concise way as follows. Let b_t be defined by the differential equation*

$$b_0 = \begin{pmatrix} 0 \\ 0 \end{pmatrix}, \quad \frac{d}{dt}b_t = - \begin{pmatrix} 0 & -\omega_t \\ \omega_t & 0 \end{pmatrix} b_t + \begin{pmatrix} u_t \\ 0 \end{pmatrix}. \quad (3)$$

Then at all times the state satisfies $R(\theta_t)^T x_t = b_t$ where $R(\theta)$ denotes the rotation of angle θ .

Proof. we have: $\frac{d}{dt} [R(\theta_t)^T x_t] = R(\theta_t)^T \left[-\omega_t J x_t + R(\theta_t) \begin{pmatrix} u_t \\ 0 \end{pmatrix} \right] = -\omega_t J R(\theta_t)^T x_t + \begin{pmatrix} u_t \\ 0 \end{pmatrix}$

where $J := \begin{pmatrix} 0 & -1 \\ 1 & 0 \end{pmatrix}$ commutes with $R(\theta_t)^T$. Thus the quantity $R(\theta_t)^T x_t$ satisfies (3). \square

The physical interpretation of the proposition is clear: Assume for the sake of simplicity that $\omega_t \equiv 0$. This means the car moves along a straight line, and the condition of Proposition 2 becomes $x_t = R(\theta_t)(\alpha(t), 0)^T = R(\theta_0)(\alpha(t), 0)^T$ where $\alpha(t) = \int_0^t u_s ds$ is the total traveled distance according to the odometer, that is, the car belongs to a circle centered at the initial position and of radius $\alpha(t)$. Let us see now whether a nonlinear counterpart of Proposition 1 might hold for the extended Kalman filter (EKF).

2.3 EKF equations

In the latter problem, the initial position is assumed to be known but the not the heading, so we let initially $\hat{x}_0 = 0_{2,1}$. The initial covariance matrix must reflect dispersion only on the heading angle, so we let it be equal to, e.g.,

$$P_0 = \begin{pmatrix} \pi/2 & 0 & 0 \\ 0 & 0 & 0 \\ 0 & 0 & 0 \end{pmatrix}.$$

Of course, after a few time steps the position becomes also uncertain due to the initial heading error but Proposition 2 holds. The standard EKF equations for the continuous time with discrete observations system considered in Section 2.2 rely on a propagation step between two observations, and an update step at each measurement time.

Propagation:

$$\begin{aligned} \frac{d}{dt} \hat{\theta}_t &= \omega_t, \\ \frac{d}{dt} \hat{x}_t &= \begin{pmatrix} \cos \hat{\theta}_t \\ \sin \hat{\theta}_t \end{pmatrix} u_t, & t_{n-1} < t < t_n, \\ \frac{d}{dt} P_t &= A_t P_t + P_t A_t^T, & t_{n-1} < t < t_n, \end{aligned} \quad (4)$$

with

$$A_t = \begin{pmatrix} 0 & 0 & 0 \\ -\sin(\hat{\theta}_t)u_t & 0 & 0 \\ \cos(\hat{\theta}_t)u_t & 0 & 0 \end{pmatrix}.$$

Note that Equation (4) contains no process noise (usually denoted by Q_t) due to deterministic dynamics.

Update: The update consists of the following steps:

- Computation of the gain:

$$K_n = P_{t_n} H^T (H P_{t_n} H^T + R)^{-1},$$

with $H = \begin{pmatrix} 0 & 1 & 0 \\ 0 & 0 & 1 \end{pmatrix}$.

- Computation of the innovation:

$$z = Y_n - \hat{x}_{t_n}.$$

- Computation of the new estimate:

$$\begin{pmatrix} \hat{\theta}_{t_n}^+ \\ \hat{x}_{t_n}^+ \end{pmatrix} = \begin{pmatrix} \hat{\theta}_{t_n} \\ \hat{x}_{t_n} \end{pmatrix} + K_n z.$$

- Update of the covariance matrix:

$$P_{t_n}^+ = (I - K_n H) P_{t_n}.$$

Due to the update, we see no reason why the EKF estimates should remain in the submanifold defined at Proposition 2. Simulations below will confirm this indeed. But before that, let us study what happens with the IEKF for the considered problem.

3 Invariant filtering with perfect odometry

The considered system is left-invariant on the Lie group $SE(2)$ [4]. A Left-invariant IEKF for our system is based on the error variable:

$$\begin{pmatrix} \hat{\theta} - \theta \\ R(\theta)^T (\hat{x}_t - x_t) \end{pmatrix}, \quad (5)$$

hence its name: the error variable is invariant to left multiplications on $SE(2)$ (that is change of global frame) which write $\theta \rightarrow \theta + \alpha$, $x \rightarrow R(\alpha)x$. As a result, the covariance matrix P_t output by the IEKF is an approximation to the dispersion of this invariant error.

3.1 IEKF equations

The IEKF equations for the considered example has already been derived in [1] and are based on a propagation and an update step as follows:

Propagation:

$$\begin{aligned} \frac{d}{dt} \hat{\theta}_t &= \omega_t, \\ \frac{d}{dt} \hat{x}_t &= \begin{pmatrix} \cos \hat{\theta}_t \\ \sin \hat{\theta}_t \end{pmatrix} u_t, \\ \frac{d}{dt} P_t &= A_t P_t + P_t A_t^T, \end{aligned} \quad t_{n-1} < t < t_n, \quad (6)$$

with

$$A_t = \begin{pmatrix} 0 & 0 & 0 \\ 0 & 0 & \omega_t \\ -u_t & -\omega_t & 0 \end{pmatrix}.$$

Again, the equation contains no process noise.

Update: The update consists of the following steps:

- Computation of the gain:

$$K_n = P H^T (H P H^T + R)^{-1},$$

$$\text{with } H = \begin{pmatrix} 0 & 1 & 0 \\ 0 & 0 & 1 \end{pmatrix}.$$

- Computation of the innovation:

$$z = R(\hat{\theta}_{t_n})^T (Y_n - \hat{x}_{t_n}).$$

- Computation of the new estimate:

$$\begin{pmatrix} R(\hat{\theta}_{t_n}^+) & \hat{x}_{t_n}^+ \\ 0_{1 \times 2} & 1 \end{pmatrix} = \begin{pmatrix} R(\hat{\theta}_{t_n}) & \hat{x}_{t_n} \\ 0_{1 \times 2} & 1 \end{pmatrix} \exp(K_n z) \quad (7)$$

where $\exp : \mathbb{R}^3 \rightarrow \mathbb{R}^3$ is the exponential map of the Lie group $SE(2)$ defined for $\theta \in \mathbb{R}$, $x \in \mathbb{R}^2$ by

$$\exp \begin{pmatrix} \theta \\ x \end{pmatrix} = \begin{pmatrix} R(\theta) & B(\theta)x \\ 0_{1 \times 2} & 1 \end{pmatrix},$$

$$\text{with } B(\theta) = \frac{1}{\theta} \begin{pmatrix} \sin \theta & -(1 - \cos \theta) \\ (1 - \cos \theta) & \sin \theta \end{pmatrix}.$$

- Update of the covariance matrix:

$$P_{t_n}^+ = (I - K_n H) P_{t_n}. \quad (8)$$

with initial values such as in Section 2.3. The IEKF is a left-invariant observer in the sense of [4]: the output error and the gains are computed in the frame of the car, making them insensitive to change of global frame (i.e. left group multiplications). However, it has the additional property of being an EKF variant, and as such its tuning is optimal for the noisy problem up to second order terms.

3.2 Implications of perfect odometry for the IEKF

It turns out that, quite surprisingly, a counterpart of Proposition 1 can be derived for the IEKF. Indeed, Proposition 2 shows the true state lives in a one-dimensional manifold defined at all times by $R(\theta_t)^T x_t = b_t$. The following result shows that whatever the initial heading error, the IEKF output estimate lives in this very manifold too. The proof has been moved to the Appendix.

Theorem 1. *The IEKF estimate as defined just above satisfies at all times $R(\hat{\theta}_t)^T \hat{x}_t = b_t$ with b_t defined at eq (3) and thus lives in the same one-dimensional manifold as the state space whatever the initial heading value $\hat{\theta}_0$.*

3.3 Numerical illustration of the theorem

To fix ideas, assume to car is moving along a straight line, i.e. $\omega_t \equiv 0$. In this case the theorem implies $\hat{x}_t = R(\hat{\theta}_t)(\alpha(t), 0)$ where $\alpha(t) = \int_0^t u_s ds$ is the distance traveled according to the odometer. This implies the two physically logical to expect properties of the estimate, that are yet never met by the standard EKF:

1. Despite the updates applied by the IEKF to the state, the total distance traveled by the estimate matches exactly the distance given by the odometer
2. The car estimated heading is always parrallel to a ray that passes through the origin

Those properties are logical to expect since the odometer (assumed perfect) indicates the car is *necessarily* travelling along a (unknown) straight line emanating from the origin.

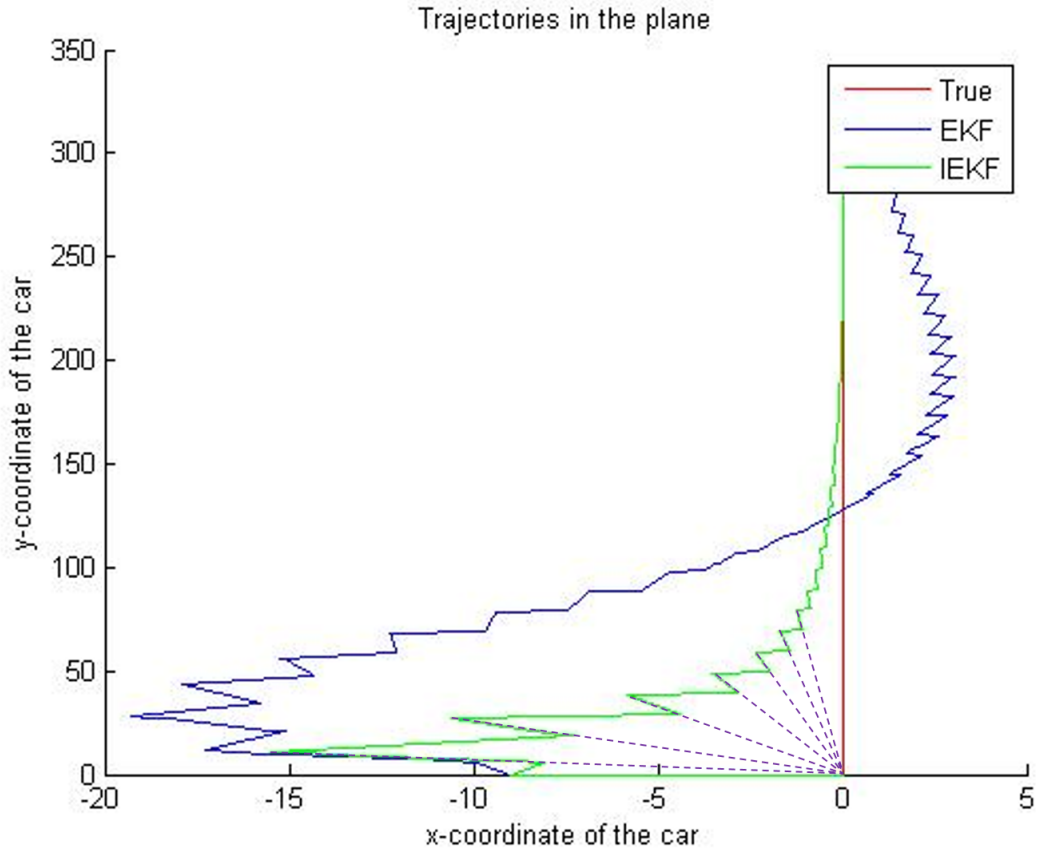


Figure 1: Illustration of Theorem 1: Car with *perfect* odometry, with *known* initial position, and *unknown* initial orientation. True and estimated trajectories (EKF and IEKF). The odometry indicates $\omega_t \equiv 0$, thus both filters move along straight lines between two updates. But the IEKF update is such that the car always moves along rays of a circle centered at the known initial position, as evidenced by the dotted segments, whereas this physical information is totally destroyed by the standard EKF updates.

Figure 1 displays the trajectory of the car for $\omega_t \equiv 0$ and the trajectories of the EKF and IEKF estimates. We see the IEKF achieves property (2) above, as evidenced by the dotted segments that prolongate the trajectory of the car between two updates.

Figure 2 displays the error between the total distance traveled by the estimate of respectively the IEKF and the EKF and the total distance traveled by the true car. Due to perfect odometry, the user can evaluate exactly the distance traveled by merely integrating the odometer measurements. We see the IEKF makes no mistake on this value whereas the EKF totally miscalculates it.

4 Implications in terms of convergence

In this section, once again for the sake of simplicity, we consider the car moves along a straight line, i.e., $\omega_t \equiv 0$.

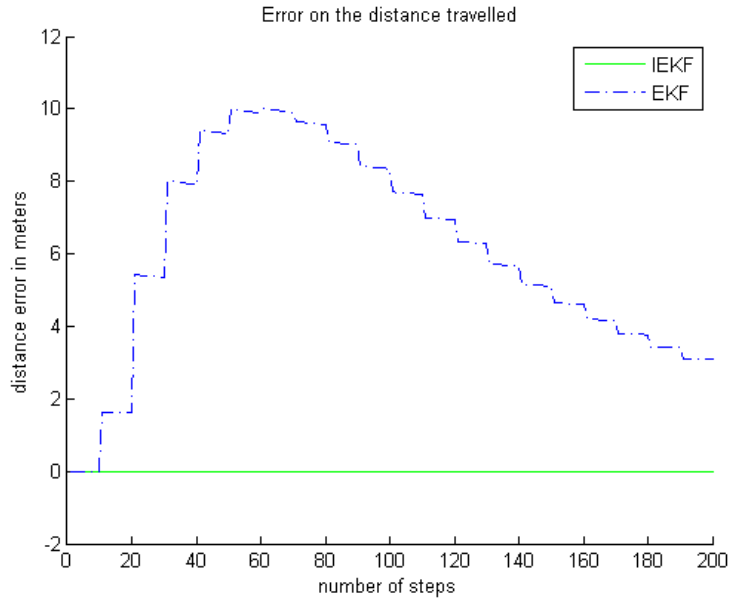


Figure 2: Error between the distance traveled by the estimate for respectively IEKF and EKF (dotted line) and the true distance traveled (according to perfect odometer). The IEKF preserves the information delivered by the odometer whereas the IEKF loses it completely.

4.1 Numerical evidence

The results of EKF and IEKF in terms of position error are displayed on Figure 3 with identical covariance matrices tuning. To obtain cleaner curves, we fed the filters with unnoisy measurements (which amounts to study their behavior when used as nonlinear observers). We see the IEKF outperforms the EKF as

- the IEKF initialized with a 40° angle error, beats the EKF initialized with a 5° angle error (top plot) !
- All EKFs (even with a 5° angle initial error) totally fail to converge (bottom plot) whereas the IEKF does.

This last feature may be explained by the fact the dynamics being deterministic, the gains tend to 0. If the EKF has failed to reduce the error enough during the transitory phase, it may fail to converge as observed here.

4.2 IEKF almost global convergence properties

The following theorem leverages the unexpected “physical” properties underlined by Theorem 1, to prove almost global convergence of the IEKF used as a non-linear observer (i.e. noise being turned off). This is a remarkable result as global convergence properties of EKFs are in general very difficult to derive (in the present case they are impossible to derive as they do not converge). The proof has been moved to the Appendix.

Theorem 2. Consider deterministic dynamics (1) with noisy output (2). Assume the observations occur at a constant rate ($t_n = n\Delta T$ with $\Delta T > 0$) with noise covariance of the form $R = rI_2$ with $r > 0$. Assume that the initial position is known and equal to $0_{2,1}$ and the car is moving along a straight line with constant speed i.e., $\omega_t \equiv 0$ and $u_t \equiv 1$. Then, for any initial orientation error such that $|\hat{\theta}(0) - \theta(0)| \neq \pi \pmod{2\pi}$ the IEKF used as a nonlinear observer globally converges to the true state. Moreover, we have the following convergence rates : $\hat{\theta}_{t_n} - \theta_{t_n} \sim C/n^3$ and $\hat{x}_{t_n} - x_{t_n} \sim C/n^2$ for some $C > 0$.

References

- [1] Axel Barrau and Silvère Bonnabel. The invariant extended kalman filter as a stable observer. *arXiv preprint arXiv:1410.1465*, 2014.
- [2] Axel Barrau and Silvere Bonnabel. Intrinsic filtering on lie groups with applications to attitude estimation. *IEEE Transactions on Automatic Control*, 60(2):436 – 449, 2015.
- [3] Pedro Batista, Carlos Silvestre, and Paulo Oliveira. Attitude and earth velocity estimation-part i: Globally exponentially stable observer. In *Decision and Control (CDC), 2014 IEEE 53rd Annual Conference on*, pages 121–126. IEEE, 2014.
- [4] S. Bonnabel, Ph. Martin, and P. Rouchon. Non-linear symmetry-preserving observers on Lie groups. *IEEE Trans. on Automatic Control*, 54(7):1709 – 1713, 2009.
- [5] S. Bonnabel, Ph. Martin, and E. Salaun. Invariant extended Kalman filter: theory and application to a velocity-aided attitude estimation problem. In *Decision and Control, 2009 held jointly with the 2009 28th Chinese Control Conference. CDC/CCC 2009. Proceedings of the 48th IEEE Conference on*, pages 1297–1304. IEEE, 2009.
- [6] Silvere Bonnabel. Left-invariant extended kalman filter and attitude estimation. In *IEEE conference on decision and control*, pages 1027–1032, 2007.
- [7] Guillaume Bourmaud, Rémi Mégret, Audrey Giremus, and Yannick Berthoumieu. Discrete extended Kalman filter on Lie groups. In *Signal Processing Conference (EUSIPCO), 2013 Proceedings of the 21st European*, pages 1–5. IEEE, 2013.
- [8] John L Crassidis, F Landis Markley, and Yang Cheng. Survey of nonlinear attitude estimation methods. *Journal of Guidance, Control, and Dynamics*, 30(1):12–28, 2007.
- [9] Garry A Einicke, Langford B White, et al. Robust extended kalman filtering. *IEEE Transactions on Signal Processing*, 47(9):2596–2599, 1999.
- [10] D. Guillaume and P. Rouchon. Observation and control of a simplified car. In *proceedings IFAC Motion Control, Grenoble*, 1998.

- [11] Minh-Duc Hua, Guillaume Ducard, Tarek Hamel, Robert Mahony, and Konrad Rudin. Implementation of a nonlinear attitude estimator for aerial robotic vehicles. *Control Systems Technology, IEEE Transactions on*, 22(1):201–213, 2014.
- [12] Maziar Izadi and Amit K Sanyal. Rigid body attitude estimation based on the lagrange–d’alembert principle. *Automatica*, 50(10):2570–2577, 2014.
- [13] Arthur J Krener. The convergence of the extended kalman filter. In *Directions in mathematical systems theory and optimization*, pages 173–182. Springer, 2003.
- [14] Ph. Martin, E. Salaün, et al. Generalized multiplicative extended kalman filter for aided attitude and heading reference system. In *Proc. AIAA Guid., Navigat., Control Conf*, pages 1–13, 2010.
- [15] W. Park, Y. Liu, Y. Zhou, M. Moses, G. S. Chirikjian, et al. Kinematic state estimation and motion planning for stochastic nonholonomic systems using the exponential map. *Robotica*, 26(4):419–434, 2008.
- [16] F. Sonnemann Reif, K. and R. Unbehauen. An ekf-based nonlinear observer with a prescribed degree of stability. *Automatica*, 34:1119–1123, 1998.
- [17] Amit K Sanyal and Nikolaj Nordkvist. Attitude state estimation with multirate measurements for almost global attitude feedback tracking. *Journal of Guidance, Control, and Dynamics*, 35(3):868–880, 2012.
- [18] K. C. Wolfe, M. Mashner, and G. S. Chirikjian. Bayesian fusion on Lie groups. *Journal of Algebraic Statistics*, 2(1):75–97, 2011.
- [19] Mahdi Zamani, Jochen Trumpf, and Robert Mahony. On the distance to optimality of the geometric approximate minimum-energy attitude filter. In *American Control Conference (ACC), 2014*, pages 4943–4948. IEEE, 2014.

A Proof of Theorem 1

Proposition 2 proved $R(\theta_t)^T x_t = b_t$. Now let $\tilde{H}_t^e = R(\hat{\theta}_t)^T [-Jb_t, I_2]$ and let

$$M_t := \tilde{H}_t^e P_t (\tilde{H}_t^e)^T, \quad N_t := R(\hat{\theta}_t)^T \hat{x}_t - b_t$$

Our goal is to prove $N_t \equiv 0$. We have $M_0 = 0$ and $N_0 = 0$. Assume $M_{t_{n-1}} = 0$, $N_{t_{n-1}} = 0$. During the propagation step $\frac{d}{dt} N_t = 0$ by mimicking the proof of Proposition 2 and thus $N_{t_n} = 0$. Moreover

$$\frac{d}{dt} M_t = \left[\left(\frac{d}{dt} \tilde{H}_t^e \right) + \tilde{H}_t^e A_t \right] P_t \left[\left(\frac{d}{dt} \tilde{H}_t^e \right) + \tilde{H}_t^e A_t \right]^T$$

A simple computation shows $\frac{d}{dt}M_t = 0$ as:

$$\begin{aligned} \frac{d}{dt}\tilde{H}_t^e &= -\omega_t R(\hat{\theta}_t)^T J [-Jb_t, I_2] \\ + R(\hat{\theta}_t)^T \left[-J^2\omega_t b_t + J \begin{pmatrix} u \\ 0 \end{pmatrix}, 0_2 \right] &= R(\hat{\theta}_t)^T J \left[\begin{pmatrix} u \\ 0 \end{pmatrix}, -\omega_t I_2 \right] \\ \tilde{H}_t^e A_t &= R(\hat{\theta}_t)^T [-Jb_t, I_2] \begin{pmatrix} 0 & 0 & 0 \\ 0 & 0 & -\omega_t \\ -u_t & \omega_t & 0 \end{pmatrix} \\ &= R(\hat{\theta}_t)^T \left[-J \begin{pmatrix} u \\ 0 \end{pmatrix}, J\omega_t \right] \end{aligned}$$

and thus $M_{t_n} = 0$. As P_t is symmetric this means $H_{t_n}^e P_{t_n} = 0$, proving that $[-Jb_{t_n}, I_2]^T$ defines a basis of the orthogonal space to $\text{Im } P_{t_n}$ and thus to $\text{Im } K_n$. This implies the image of K_n is spanned by $w := \begin{pmatrix} 1 \\ Jb_{t_n} \end{pmatrix}$. Let us now focus on (7). We have just proved $K_n z = \alpha w$ with $\alpha \in \mathbb{R}$ that we assume equal to 1 without loss of generality. It follows directly from the definition of the Lie exponential map on $SE(2)$ that $\hat{\theta}^+, \hat{x}^+$ defined by (7) are the solution at $s = 1$ to the equation

$$\frac{d}{ds}\tilde{\theta}(s) = 1, \quad \frac{d}{ds}\tilde{x}(s) = R(\tilde{\theta}(s))Jb_{t_n}, \quad (\tilde{\theta}(0), \tilde{x}(0)) = (\hat{\theta}_{t_n}, \hat{x}_{t_n})$$

Let $a(s) := R(\tilde{\theta}(s))^T \tilde{x}(s)$. We have then $\frac{d}{ds}a(s) = -JR(\tilde{\theta}(s))^T \tilde{x}(s) + Jb_{t_n} = J(-a(s) + b_{t_n})$. As $a(0) - b_{t_n} = 0$ this implies $a(s) - b_{t_n} \equiv 0$ and in particular $a(1) = b_{t_n}$.

We have thus proved that $N_{t_n}^+ = N_{t_n} = 0$. To complete the induction over n , we must check also that $M_{t_n}^+ = M_{t_n} = 0$. Note that $M_t = 0$ is equivalent to $[-Jb_t, I_2]^T P_t = 0$. As N_t is preserved by the update, so is b_t . Thus $(\tilde{H}_{t_n}^e)^+ P_{t_n}^+ (\tilde{H}_{t_n}^e)^+{}^T = 0$ as $[-Jb_t, I_2]^T P_{t_n}^+ = [-Jb_t, I_2]^T (I - K_n H) P_{t_n} = [-Jb_t, I_2]^T P_{t_n} \cdots = 0$.

B Proof of Theorem 2

The solution of the Riccati equation (6),(8) reads

$$P_t = \begin{pmatrix} a(t) & 0 & ta(t) \\ 0 & 0 & 0 \\ ta(t) & 0 & t^2 a(t) \end{pmatrix}, \quad P_{t_n^+} = \begin{pmatrix} a(t_n^+) & 0 & t_n a(t_n^+) \\ 0 & 0 & 0 \\ t_n a(t_n^+) & 0 & t_n^2 a(t_n^+) \end{pmatrix}, \quad (9)$$

with $a(0) = p_0$, $\frac{d}{dt}a(t) = 0$ during the propagation ($t \in]t_{n-1}, t_n]$) and

$$a(t_n^+) = a(t_n) - \frac{t_n^2 a(t_n)^2}{r + t_n^2 a(t_n)} \quad (10)$$

at the update steps. Checking this value of P_t verifies (6),(8) is straightforward.

Now we compute the value of $a(t)$ for any t . Eq. (10) can be re-written $\frac{1}{a(t_n)^+} = \frac{1}{a(t_n)} + \Delta T^2 \frac{n^2}{r}$, where t_n has been replaced with $n\Delta T$. As we have $a(t_n^+) = a(t_{n+1})$ we can apply the square pyramidal number formula to obtain:

$$\frac{1}{a(t_n)^+} = \frac{1}{p_0} + \frac{\Delta T^2}{r} \frac{n(n+1)(2n+1)}{6}. \quad (11)$$

In turn, let us write a recursive equation verified by the heading error $\tilde{\theta}_t = \hat{\theta}_t - \theta_t$. We will need the update function of $\hat{\theta}_{t_n}$ (extracted from eq. (7)):

$$\hat{\theta}_{t_n}^+ = \hat{\theta}_{t_n} + K_n(1, :)z, \quad (12)$$

where we have to compute $K_n(1, :)$ (first line of the gain matrix) and z . First, using the expression of P_t , we can write the first line of the gain K_n :

$$K_n(1, :) = \left(0, \frac{t_n a(t_n)}{t_n^2 a(t_n) + r} \right). \quad (13)$$

Then we write the innovation as a function of the heading error $\tilde{\theta}_t$. As we have $\omega_t = 0$ and $u_t = Cste = u$, Proposition 2 boils down to the relation $x_t = R(\theta_t)(tu, 0)^T$. Following Theorem 1 we also have at all time: $\hat{x}_t = R(\hat{\theta}_t)(tu, 0)^T$, which allows writing the innovation as a function of $\tilde{\theta}_t$:

$$z = tu \left(\cos(\tilde{\theta}_t) - 1, -\sin(\tilde{\theta}_t) \right)^T. \quad (14)$$

Putting together (13) and (14) we obtain:

$$\tilde{\theta}_{t_{n+1}} = \tilde{\theta}_{t_n} - \alpha_n \sin(\tilde{\theta}_{t_n}), \quad (15)$$

with $\alpha_n = \frac{t_n^2 a(t_n)}{t_n^2 a(t_n) + r}$. As a first consequence, $|\tilde{\theta}_t|$ is decreasing. Thus, $\frac{\sin(x)}{x}$ being decreasing on $[0, \pi]$, we have $\frac{\sin(\theta_t)}{\theta_t} \geq \frac{\sin(\theta_0)}{\theta_0}$, i.e. $\sin(\theta_t) \geq \frac{\sin(\theta_0)}{\theta_0} \theta_t$. Introducing the latter inequality into (15) we obtain $\tilde{\theta}_{t_{n+1}} \leq \tilde{\theta}_{t_n} \left(1 - \alpha_n \frac{\sin(\theta_0)}{\theta_0} \right)$, i.e. $\log(\tilde{\theta}_{t_n}^+) \leq \log(\tilde{\theta}_{t_n}) + \log\left(1 - \alpha_n \frac{\sin(\theta_0)}{\theta_0}\right) \leq \log(\tilde{\theta}_{t_n}) - \alpha_n \frac{\sin(\theta_0)}{\theta_0}$. As using (11) we have $\alpha_n = 3/n + \mathcal{O}(1/n^2)$, this proves $\theta_{t_n} = \mathcal{O}\left(1/n^{3\frac{\sin(\theta_t)}{\theta_t}}\right)$. But (15) also leads to $\log(\tilde{\theta}_{t_{n+1}}(n+1)^3) - \log(\tilde{\theta}_{t_n} n^3) = \log\left(1 - \alpha_n \frac{\sin(\theta_{t_n})}{\theta_{t_n}}\right) + 3\log(1+1/n)$. Using $\alpha_n \frac{\sin(\theta_{t_n})}{\theta_{t_n}} = (3/n + \mathcal{O}(1/n^2)) \left(1 - \frac{1}{6n^{2 \times 3 \frac{\sin(\theta_t)}{\theta_t}}}\right)$ we obtain

$$\log(\tilde{\theta}_{t_{n+1}}(n+1)^3) - \log(\tilde{\theta}_{t_n} n^3) = \mathcal{O}\left(1/n^{1+2 \times 3 \frac{\sin(\theta_t)}{\theta_t}}\right)$$

thus $\log(\tilde{\theta}_{t_{n+1}}(n+1)^3)$ is convergent, and there exists $C > 0$ such that $\tilde{\theta}_{t_{n+1}} \sim C/(n+1)^3$. And Theorem 1 implies $\hat{x}_t - x_t \sim tu\tilde{\theta}_t$ which is of order C/n^2 at $t = t_n$.

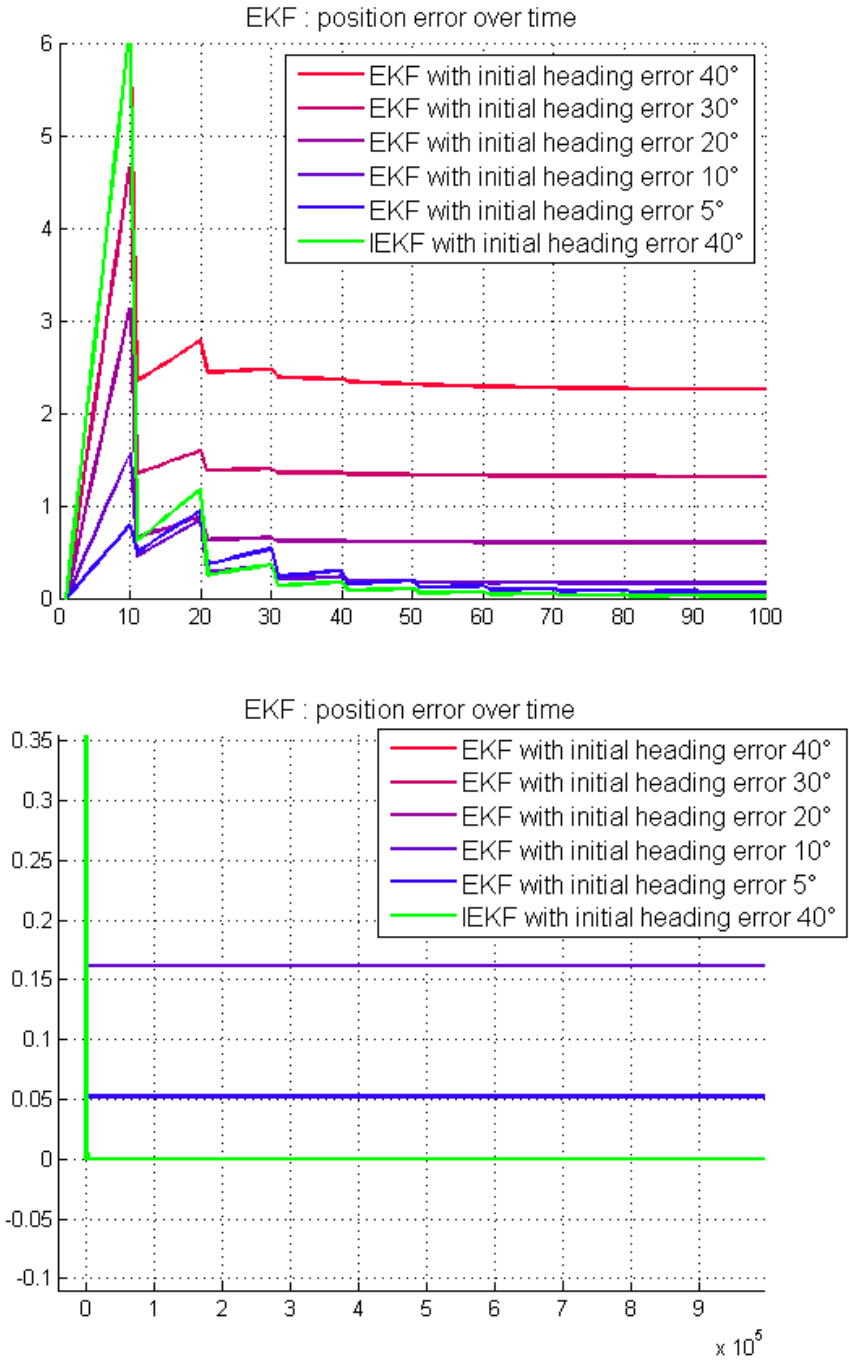


Figure 3: Influence of singular information: Position error of the EKF for GPS and perfect odometry, with initial position known and initial heading unknown. Top plot: We see the IEKF initialized with a large error (40°) even beats the EKF initialized with a small error (5°). Bottom plot : Vertical zoom and extended running time (1 million steps). The EKF errors stabilize at a non-zero value whereas the IEKF error goes to 0.